INFECTION AND IMMUNITY, May 2007, p. 2101–2109 Vol. 75, No. 5
0019-9567/07/$08.00+0 doi:10.1128/IAI.01515-06

Pet, a Non-AB Toxin, Is Transported and Translocated into Epithelial Cells by a Retrograde Trafficking Pathway▽

Fernando Navarro-García,[1]* Adrián Canizalez-Roman,[1] Kaitlin E. Burlingame,[2] Ken Teter,[2] and Jorge E. Vidal[1]

Department of Cell Biology, Centro de Investigación y de Estudios Avanzados (Cinvestav-Zacatenco), Ap. Postal 14-740, 07000 México, DF, Mexico,[1] and Biomolecular Science Center and Department of Molecular Biology and Microbiology, University of Central Florida, 12722 Research Parkway, Orlando, Florida 32826[2]

Received 20 September 2006/Returned for modification 9 November 2006/Accepted 5 February 2007

The plasmid-encoded toxin (Pet) of enteroaggregative *Escherichia coli* is a 104-kDa autotransporter protein that exhibits proteolytic activity against the actin-binding protein α-fodrin. Intracellular cleavage of epithelial fodrin by Pet disrupts the actin cytoskeleton, causing both cytotoxic and enterotoxic effects. Intoxication requires the serine protease activity of Pet and toxin endocytosis from clathrin-coated pits. The additional events in the intracellular trafficking of Pet are largely uncharacterized. Here, we determined by confocal microscopy that internalized Pet is transferred from the early endosomes to the Golgi apparatus and then travels to the endoplasmic reticulum (ER). Pet associates with the Sec61p translocon before it moves into the cytosol as an intact, 104-kDa protein. This translocation process contrasts with the export of other ER-translocating toxins, in which only the catalytic A subunit of the AB toxin enters the cytosol. However, like intoxication with these AB toxins, Pet intoxication was inhibited in a subset of mutant CHO cell lines with aberrant activity in the ER-associated degradation pathway of ER-to-cytosol translocation. This is the first report which documents the cell surface-to-ER and ER-to-cytosol trafficking of a bacterial non-AB toxin.

Plasmid-encoded toxin (Pet), a 104-kDa protein secreted by enteroaggregative *Escherichia coli*, damages the human intestinal mucosa by inducing exfoliation of epithelial cells and development of crypt abscesses (23). This toxin is classified as a serine protease autotransporter protein of the *Enterobacteriaceae* (SPATE) (10). Autotransporters comprise a special group of virulence-associated proteins that are secreted by gram-negative bacteria and have diverse biological functions (9, 11). Each SPATE contains three domains: (i) an amino-terminal leader peptide (signal sequence); (ii) the secreted "mature" protein (passenger domain); and (iii) a carboxy-terminal domain (translocation unit) which forms a β-barrel pore through which the passenger protein is secreted. All SPATEs also possess a conserved serine protease motif with the consensus sequence GDSGSP (11).

The eukaryotic target of Pet is fodrin, a cytosolic actin-binding protein. Fodrin cleavage disrupts the organization of the actin cytoskeleton and leads to contraction of the cytoskeleton (1), loss of actin stress fibers, and release of focal contacts in HEp-2 and HT29/C1 cell monolayers. These cytotoxic effects eventually result in cell rounding and detachment from the substratum (24). Enterotoxicity results from similar cellular effects in the intestinal epithelium (23). As Pet intoxication is blocked by the serine protease inhibitor phenylmethylsulfonyl fluoride and by an S260I mutation in the active site of the Pet serine protease motif, the cytotoxic and enterotoxic effects of Pet depend upon its serine protease activity (24).

Pet intoxication also requires toxin endocytosis to reach the intracellular target. We have recently found that Pet binds to the epithelial cell surface and is internalized by clathrin-coated vesicles (F. Navarro-Garcia, A. Canizalez-Roman, J. E. Vidal, and M. I. Salazar, submitted for publication). Other studies have shown that brefeldin A (BfA) inhibits the cytotoxic effects of Pet by disrupting its intracellular trafficking (22). These data suggest that Pet may exploit the vesicular trafficking pathways of the target cell in order to reach its cytosolic target.

Many plant and bacterial toxins use the eukaryotic secretory pathway to enter the host cell cytoplasm (19, 28). These toxins have an AB structure that consists of a catalytic A moiety and a receptor-binding B moiety. Some AB toxins enter cells by receptor-mediated endocytosis and pass directly from acidified endosomes to the cytosol. Diphtheria toxin (DT) and other toxins in this category undergo an acid-dependent conformational change which generates a pore in the endosomal membrane that facilitates A-chain access to the cytosol (26). Other AB toxins, such as cholera toxin (CT), require further trafficking and travel from the endosomes to the Golgi apparatus en route to an endoplasmic reticulum (ER) exit site (17). The A chains of these ER-translocating toxins masquerade as misfolded proteins in order to promote their export into the cytosol through the quality control mechanism of ER-associated degradation (ERAD). Export by this route also involves the Sec61p translocon, a gated pore in the ER membrane (27). For both endosomal and ER translocation sites, AB subunit dissociation precedes or occurs concomitantly with A-chain passage into the cytosol.

Pet is not an AB toxin, yet preliminary studies suggested that it could follow an AB toxin trafficking pathway from the cell surface to the ER and from the ER to the cytosol. To better characterize the intracellular trafficking and translocation

* Corresponding author. Mailing address: Department of Cell Biology, Cinvestav-Zacatenco, Ap. Postal 14-740, 07000 México, DF, Mexico. Phone: (525) 5061-3990. Fax: (525) 5061-3393. E-mail: fnavarro@cell.cinvestav.mx.

▽ Published ahead of print on 12 February 2007.

routes of Pet, we used confocal microscopy to document Pet transport from the early endosomes to the Golgi apparatus and from the Golgi apparatus to the ER. Pet associated with the Sec61p translocon in the ER and then entered the cytosol as an intact, 104-kDa protein. Functional assays confirmed an ER exit site for Pet, since Pet intoxication was inhibited by aberrant ERAD activity but not by endosomal alkalization. This is the first report to demonstrate cell surface-to-ER trafficking and ER-to-cytosol translocation of a bacterial non-AB toxin.

MATERIALS AND METHODS

Materials, antibodies, and bacterial strains. Unless otherwise noted, all chemicals and other reagents were purchased from Sigma-Aldrich, Inc. (St. Louis, MO).

Mouse anti-Pet polyclonal antibodies were prepared for this study by immunizing mice with the 104-kDa Pet protein excised from a sodium dodecyl sulfate (SDS)-polyacrylamide gel electrophoresis (PAGE) gel. Rabbit anti-Pet antibodies have been described previously (23); mouse anti-early endosome antigen 1 (EEA-1) monoclonal antibodies were obtained from Transduction Laboratories (Lexington, KY); mouse anti-lysosome associated membrane protein 1 (LAMP-1) monoclonal antibodies were obtained from Pharmigen (San Diego, CA); rabbit anti-calnexin antibodies were obtained from Calbiochem (San Diego, CA); goat anti-α-fodrin antibodies were obtained from Santa Cruz Biotech (Santa Cruz, CA); rabbit anti-Sec61α antibodies were obtained from Affinity BioReagents, Inc. (Golden, CO); rabbit anti-CT antibodies were obtained from Sigma-Aldrich, Inc.; and rabbit anti-cadherin antibodies were obtained from Zymed Lab, Inc. (San Francisco, CA). All conjugated secondary antibodies were purchased from Zymed Lab, Inc.

The minimal Pet clone pCEFN1 was constructed by cloning the *pet* gene of enteroaggregative *E. coli* strain 042 into the BamHI/KpnI site of pSPORT1 as previously described (4). *E. coli* strain HB101 was transformed with pCEFN1 and maintained on L-agar or in L-broth containing 100 μg/ml ampicillin (4). To obtain the Pet protein, broth cultures of HB101(pCEFN1) were incubated overnight at 37°C and then centrifuged at 7,000 × *g* for 15 min. The culture supernatant was filtered through 0.22-μm cellulose acetate membrane filters (Corning, Cambridge, MA), concentrated 100-fold with an ultrafree centrifugal filter device with a 100-kDa cutoff (Millipore, Bedford, MA), filter sterilized again, and stored at −20°C for up to 3 months (24). Culture media from non-Pet-expressing strain HB101(pSPORT1) was concentrated as described above and used as a negative control for immunofluorescence and toxicity assays.

Cell culture. HEp-2 cells were propagated in a humidified 5% CO_2–95% air atmosphere at 37°C in Dulbecco's modified Eagle's medium supplemented with 5% fetal bovine serum (HyClone, Logan, UT), 1% nonessential amino acids, 5 mM L-glutamine, penicillin (100 U/ml), and streptomycin (100 μg/ml). Mutant and wild-type CHO cells were propagated in a humidified 5% CO_2–95% air atmosphere at 37°C in Ham's F-12 medium (GIBCO BRL, Grand Island, NY) supplemented with 10% fetal bovine serum (GIBCO BRL) and penicillin/streptomycin. The subcultures were serially propagated after they were harvested with 10 mM EDTA and 0.25% trypsin (GIBCO BRL) in phosphate-buffered saline (PBS) (pH 7.4). For fluorescence and immunoprecipitation experiments, subconfluent HEp-2 cells were resuspended with EDTA-trypsin, plated into eight-well LabTek slides (VWR, Bridgeport, NJ), and allowed to grow for ~24 h to 70% confluence before use. For the cell rounding and cell detachment assays, CHO cells were plated into 24-well plates and allowed to grow for ~24 h to 40 to 80% confluence before use.

Fluorescence assays. Pet was diluted directly into tissue culture medium without antibiotics or serum at a final concentration of 37 μg/ml. It was then added to the target cells using 250 μl (final volume) per well in eight-well LabTek slides. Following incubation in a humidified atmosphere containing 5% CO_2 and 95% air at 37°C for the times indicated below, the medium was aspirated, the cells were washed twice with PBS, and 2% formalin in PBS was added for 20 min at room temperature. The fixed cells were then permeabilized by adding 0.2% Triton X-100 in PBS for 5 min at room temperature.

Actin filaments in the permeabilized cells were visualized by incubation with 0.05 μg/ml tetramethyl rhodamine isocyanate (TRITC)-phalloidin for 30 min at room temperature. The Golgi apparatus in permeabilized cells was visualized by incubation with 5 μM BODIPY FL C5-ceramide-bovine serum albumin complexes in Hanks' buffered salt solution–10 mM HEPES (pH 7.4) for 30 min at 4°C. Rhodamine-conjugated Pet was obtained by following the instructions of the manufacturer (Sigma-Aldrich, Inc., St. Louis, MO). Proteins other than actin were visualized by incubation with the appropriate primary antibodies for 1 h at room temperature, followed by incubation for 1 h at room temperature with the secondary antibodies. Slides were mounted on Gelvatol, covered with a glass coverslip, and examined with a Leica TCS SP2 confocal microscope at a magnification of ×100.

The drug treatments for the experimental protocol described above consisted of 30 min of preincubation with 10 μM or 10 nM wortmannin or with 40 mM NH_4Cl. Pet was then added to the cells for 3 h in the presence of the drug.

Immunoprecipitation assays. Cultured HEp-2 cells in cell culture dishes (60 by 15 mm) were incubated with 37 μg Pet/ml for different times at 37°C. Cells were washed with cold PBS, resuspended in 1 ml of cold lysis buffer (50 mM Tris-HCl–150 mM NaCl [pH 7.5] containing 1% Nonidet P-40, 0.5% sodium deoxycholate, and Complete protease inhibitors), and detached by using a policeman. Cells were placed in a 1.5-ml microtube and lysed by passing them through a syringe with a 27-gauge needle. Lysed cells (500 μg) were centrifuged at 12,000 × *g* for 10 min at 4°C, and the supernatant was placed in a new 1.5-ml microtube. To perform the immunoprecipitation assay, the supernatant was incubated with anti-Sec61α (2 μg), anti-Pet (2 μg), or anti-cadherin (5 μg) antibody with slight agitation for 3 h at 4°C. Then 5 μl of a protein A-agarose suspension (Roche Diagnostics, Mannheim, Germany) was added for 3 h at 4°C. The complexes were collected by centrifugation at 12,000 × *g* for 20 s, and the supernatant was removed. The pellet was washed five times with cold PBS containing Complete protease inhibitors. The agarose pellet was resuspended in 2× gel loading buffer, the samples were boiled for 5 min, and the immunocomplexes were resolved by SDS-PAGE. The resulting protein bands were transferred to nitrocellulose membranes (35), which were probed with rabbit anti-Pet antibodies at a dilution of 1:200 or anti-cadherin antibodies at a dilution of 1:50 in PBS. Antigen-antibody reactions were visualized using horseradish peroxidase-labeled goat anti-rabbit immunoglobulin G (IgG) antibodies and were developed using the "Luminol" chemiluminescence reagent from Santa Cruz Biotech. The immunoprecipitation of Sec61α and the immunoprecipitation of cadherin were confirmed in control Western blots.

Cell rounding and cell detachment assays. Pet (40 μg/ml) was added to Ham's F-12 medium supplemented with 10% fetal bovine serum and penicillin/streptomycin. Either toxin-free medium or Pet-containing medium (250 μl) was then added to cells seeded in a 24-well plate. After 10 h of incubation, pictures were taken at magnification ×10 with a digital camera mounted on a Zeiss (Gottingen, Germany) Axiovert 25 microscope. In separate experiments the detached cells in the media were collected after 20 h of incubation, and the remaining adherent cells were collected by trypsin-EDTA treatment. Duplicate hemocytometer counts were used to determine the numbers of detached and adherent cells. The percentage of detached cells was calculated by dividing the number of detached cells by the total number of detached and adherent cells. This value obtained with control cells incubated without toxin was treated as a background value and therefore was subtracted from the corresponding value obtained with toxin-treated cells. The results are expressed below as the ratio of the experimental value to the control value, where the experimental value is the percentage of detached cells obtained with the mutant cell lines or *N*-acetyl-Leu-Leu-Norleu-Al (ALLN)-treated cells and the control value is the percentage of detached cells obtained with the wild-type CHO cells. A ratio greater than 1 indicates that the level of toxin sensitivity is higher than the level of toxin sensitivity observed with the control cells; a ratio of 1 indicates that the level of toxin sensitivity is the same as the level of toxin sensitivity observed with the control cells; and a ratio less than 1 indicates that the level of toxin resistance is higher than the level of toxin resistance observed with the control cells.

Cell fractionation. HEp-2 cells grown in 60-mm petri dishes were treated with the Pet protein for the times indicated below. Cells were delicately washed three times with ice-cold PBS (pH 7.4) and scraped into a buffer consisting of Tris-HCl (pH 7.5) (0.25 M), phenylmethylsulfonyl fluoride (50 μg/ml), aprotinin (0.5 μg/ml), and EDTA (0.5 μM). Then the cells were lysed by three freeze-thaw cycles (5 min of incubation in a dry ice-ethanol bath and 3 min of incubation in a thermoblock at 37°C). Cells were scraped into ice-cold PBS. The cell lysates were ultracentrifuged at 100,000 × *g* for 1 h at 4°C, and the supernatant fraction containing soluble cytoplasmic proteins was obtained. Equivalent volumes were boiled for 7 min, analyzed by SDS-PAGE, and electrotransferred to nitrocellulose membranes for Western blot analyses, essentially as described above. The identity of cellular fractions was confirmed with a mouse monoclonal anti-actin antibody (a gift from Manuel Hernández) for cytosolic proteins and with a rabbit anti-pan-cadherin polyclonal antibody for the membrane insoluble fraction. Cadherin was not detected in the supernatant fraction containing soluble cytoplasmic proteins.

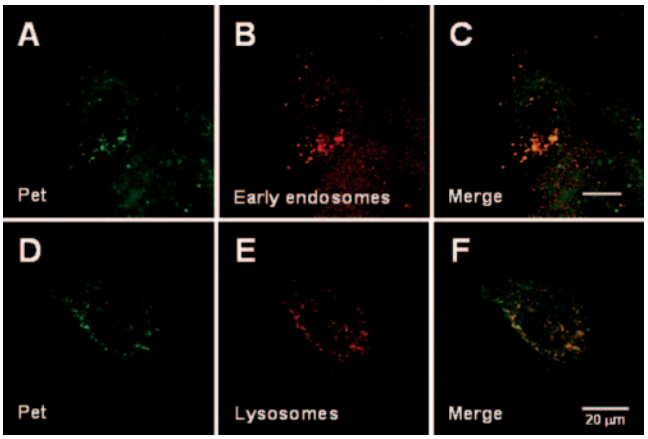

FIG. 1. Pet trafficking to the early endosomes and lysosomes. (A to C) HEp-2 cells exposed to 37 μg Pet/ml for 8 min at 37°C were fixed and permeabilized. Pet was visualized with a combination of rabbit anti-Pet antibodies and secondary fluorescein-labeled goat anti-rabbit IgG antibodies (A), while the early endosomes were visualized with a combination of mouse anti-EEA-1 antibodies and secondary rhodamine-labeled goat anti-mouse IgG antibodies (B). A merged image is shown in panel C. (D to F) HEp-2 cells exposed to 37 μg Pet/ml for 25 min at 37°C were fixed and permeabilized. Pet was visualized with a combination of rabbit anti-Pet antibodies and secondary fluorescein-labeled goat anti-rabbit IgG antibodies (D), while the lysosomes were visualized with a combination of mouse anti-LAMP-1 antibodies and secondary rhodamine-labeled goat anti-mouse IgG antibodies (E). A merged image is shown in panel F.

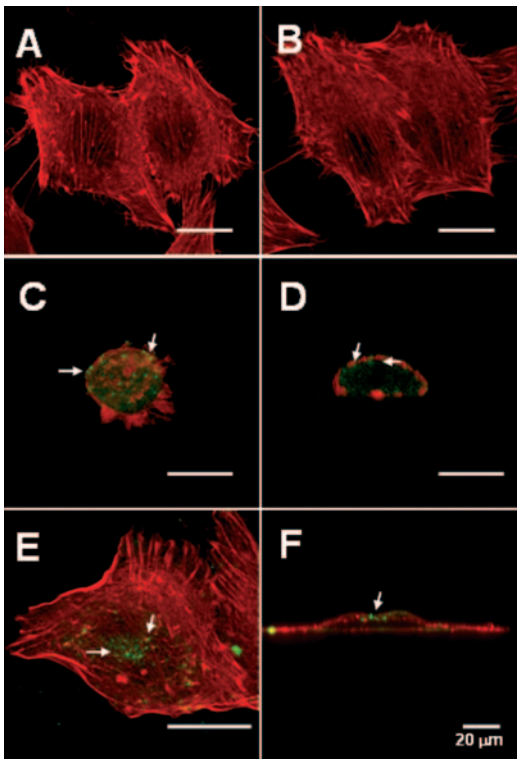

FIG. 2. Inhibition of PI 3-kinase blocks Pet trafficking and intoxication. (A and B) Untreated HEp-2 cells (A) and HEp-2 cells incubated with 10 μM wortmannin for 3.5 h at 37°C (B) were fixed, permeabilized, and stained with rhodamine-phalloidin. (C to F) HEp-2 cells preincubated for 30 min at 37°C in the absence (C and D) or in the presence (E and F) of 10 μM wortmannin were subsequently exposed to 37 μg Pet/ml for 3 h in the absence or presence of wortmannin. Similar results were obtained by using 10 nM wortmannin. The cells were then fixed, permeabilized, and stained with rhodamine-phalloidin. Pet was visualized with a combination of rabbit anti-Pet antibodies and secondary fluorescein-labeled goat anti-rabbit IgG antibodies. The images are merged images; vertical optical sections of panels C and E are shown in panels D and F, respectively. The arrows indicate Pet localization.

RESULTS

Pet endocytic trafficking in intoxicated epithelial cells. Pet internalization is required for intoxication, and we have recently found that Pet uptake occurs via clathrin-dependent endocytosis (Navarro-Garcia et al., submitted). To follow the endocytic trafficking of Pet, double-immunostaining experiments were performed (Fig. 1). Cells incubated with Pet for short periods of time (0 to 20 min) at 37°C were fixed, permeabilized, and incubated with antibodies against Pet and EEA-1. Fluorescein isothiocyanate (FITC)-labeled secondary antibodies were used to visualize Pet (Fig. 1A), while TRITC-labeled secondary antibodies were used to visualize EEA-1 (Fig. 1B). Punctate staining patterns were observed by confocal microscopy for both Pet and EEA-1. The merged image clearly demonstrated that Pet was present in the early endosomes after 8 min of incubation (Fig. 1C). Thus, as observed for the AB toxins (17, 19, 28, 29), Pet reaches the early endosomes after its endocytosis. When cells were incubated at 4°C to block endocytosis, no colocalization of Pet and EEA-1 was observed (not shown).

A fraction of internalized AB toxins are transported to the lysosomes and degraded in that compartment. However, the functional pool of toxin either is directly translocated from the endosomes to the cytosol (e.g., DT) (21) or is transported to the Golgi apparatus (e.g., ricin) (36). To detect Pet trafficking to the lysosomes, cells incubated with Pet for various times at 37°C were fixed, permeabilized, and incubated with antibodies against Pet and LAMP-1. FITC-labeled secondary antibodies were used to visualize Pet (Fig. 1D), while TRITC-labeled secondary antibodies were used to visualize LAMP-1 (Fig. 1E). Confocal microscopy analysis revealed that some of the internalized Pet colocalized with LAMP-1 after 25 min of incubation (Fig. 1F). However, Pet was also located in perinuclear structures that were distinct from the LAMP-1-positive vesicles. This suggested that a pool of internalized Pet was delivered to intracellular organelles other than the lysosomes.

Phosphoinositide 3-kinase (PI 3-kinase) is active in endocytic protein trafficking (18, 39), participates in the formation of multivesicular bodies (5), and is involved in the fusion of endosomes (13). These events are disrupted by wortmannin, a PI 3-kinase inhibitor (5, 13, 18). Accordingly, we used wortmannin to examine the role of PI 3-kinase in Pet trafficking (Fig. 2). HEp-2 cells preincubated in the absence or presence of wortmannin for 30 min were subsequently treated with Pet for 3 h in the absence or presence of wortmannin. Double-fluorescence experiments and confocal microscopy then documented the effect of wortmannin on Pet-induced damage to the actin cytoskeleton. Anti-Pet antibodies and FITC-labeled secondary antibodies were used to visualize Pet, whereas the actin cytoskeleton was stained with rhodamine-phalloidin. Ac-

tin stress fibers were clearly present in the untreated control cells (Fig. 2A) and in cells exposed to only wortmannin (Fig. 2B). In contrast, actin stress fibers were absent from Pet-treated cells incubated in the absence of wortmannin (Fig. 2C and D). Loss of an organized actin cytoskeleton also resulted in cell rounding. These toxic effects were not observed in Pet-treated cells that had been pre- and coincubated with wortmannin (Fig. 2E and F). In addition, as detected in vertical cell sections, Pet was found almost exclusively on the cortical actin cytoskeleton near the cell surface of wortmannin-treated cells (Fig. 2F). In the absence of wortmannin treatment, Pet was instead found inside the cells in vesicular structures located along the cells, which were observed as rounding cells (Fig. 2D). Collectively, these observations established that PI 3-kinase has a functional role in Pet endocytic trafficking and intoxication.

The A chains of some AB toxins move into the cytosol by crossing the membrane of the acidified endosome. This process can be inhibited by alkalizing the endosomal compartments with weak bases, such as NH_4Cl (19, 21, 26, 28). Accordingly, we used NH_4Cl to examine the role of acidic endosomes in Pet translocation (Fig. 3). HEp-2 cells preincubated in the absence or presence of NH_4Cl for 30 min were subsequently treated with Pet for 3 h in the absence or presence of NH_4Cl. Double-fluorescence experiments and confocal microscopy were then used to document the effect of NH_4Cl on Pet-induced damage to the actin cytoskeleton. Anti-Pet antibodies and FITC-labeled secondary antibodies were used to visualize Pet, whereas the actin cytoskeleton was stained with rhodamine-phalloidin. Actin stress fibers were absent from Pet-treated cells incubated either in the absence (Fig. 3A to C) or in the presence (Fig. 3D to F) of NH_4Cl, whereas treatment with NH_4Cl alone had no effect on the distribution of actin stress fibers (not shown). To confirm that NH_4Cl affected the function of the endosomes due to pH changes, CT was used as a positive control. We found that NH_4Cl changed the diffuse, perinuclear pattern of CT fluorescence (Fig. 3G to I) by concentrating the toxin into discrete punctate structures (Fig. 3J to L). Our NH_4Cl protocol also provided HEp-2 cells with substantial resistance to DT (not shown). These results indicated that Pet is not translocated to the cytosol from acidified endosomes and suggested that Pet must travel to other organelles before exiting the endomembrane system.

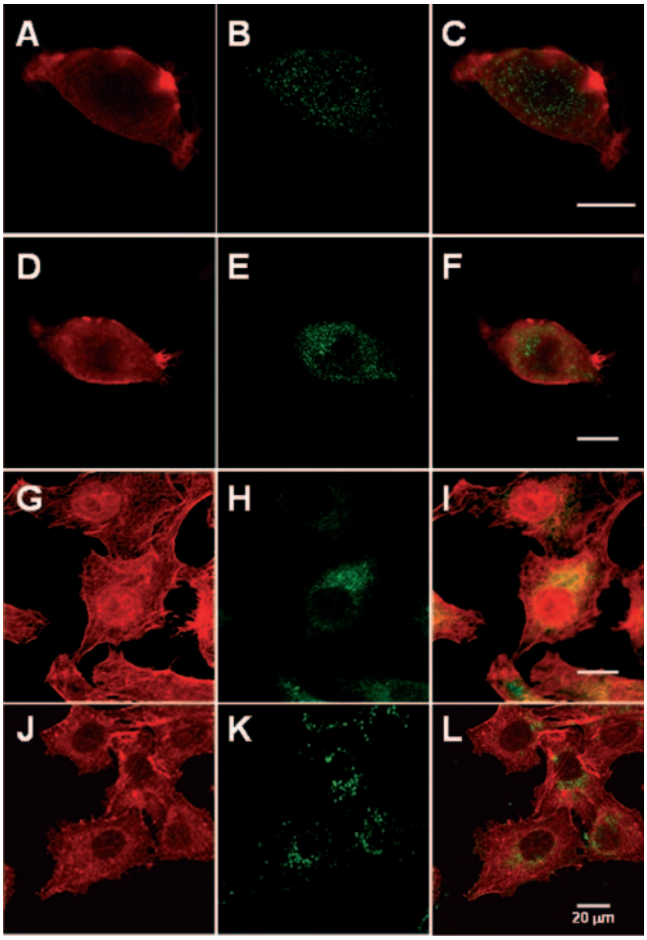

FIG. 3. Pet is not translocated to the cytosol from acidic endosomes. (A to F) HEp-2 cells preincubated for 30 min at 37°C in the absence (A to C) or in the presence (D to F) of 40 mM NH_4Cl were subsequently exposed to 37 μg Pet/ml for 3 h in the absence or presence of NH_4Cl. The cells were then fixed, permeabilized, and stained with rhodamine-phalloidin (A and D). Pet was visualized with a combination of rabbit anti-Pet antibodies and secondary fluorescein-labeled goat anti-rabbit IgG antibodies (B and E). Merged images are shown in panels C and F. (G to L) HEp-2 cells preincubated for 30 min at 37°C in the absence (G to I) or in the presence (J to L) of 40 mM NH_4Cl were subsequently exposed to 1 μg CT/ml for 3 h in the absence or presence of NH_4Cl. The cells were then fixed, permeabilized, and stained with rhodamine-phalloidin (G and J). CT was visualized with a combination of rabbit anti-CT antibodies and secondary fluorescein-labeled goat anti-rabbit IgG antibodies (H and K). Merged images are shown in panels I and L.

Retrograde transport of Pet from the Golgi apparatus to the ER. BfA induces the assimilation of the Golgi apparatus into the ER and prevents vesicular communication between the mixed ER/Golgi compartment and other organelles of the secretory pathway (3, 25, 40). Therefore, cells treated with BfA are resistant to AB-type, ER-translocating toxins. In previous work we determined that BfA also inhibits Pet intoxication (22). This suggested that Pet trafficking and intoxication require an intact Golgi apparatus. However, BfA alters endosomal morphology and endocytic trafficking as well. To determine whether Pet trafficking involves the Golgi apparatus, double-fluorescence confocal microscopy experiments were performed (Fig. 4). HEp-2 cells exposed to rhodmaine-conjugated Pet for 15, 30, or 60 min were subsequently fixed, permeabilized, and stained with BODIPY FL C5-ceramide to visualize the Golgi apparatus. In control cells that were not exposed to Pet, the Golgi apparatus appeared to be a tubulovesicular structure in the perinuclear region of the cell (Fig. 4A). This staining pattern was not altered by Pet intoxication (Fig. 4B to D). After 15 min of intoxication, Pet was found in intracellular structures that partially coincided with the Golgi apparatus (Fig. 4B). More extensive Pet colocalization with BODIPY FL C5 was observed after 30 min of intoxication (Fig. 4C), but after 60 min of incubation the toxin was no longer detected in the Golgi apparatus (Fig. 4D). These observations suggested that internalized Pet transiently accumulates in the Golgi apparatus before further trafficking, possibly to the ER.

To detect Pet transport to the ER, double-immunostaining

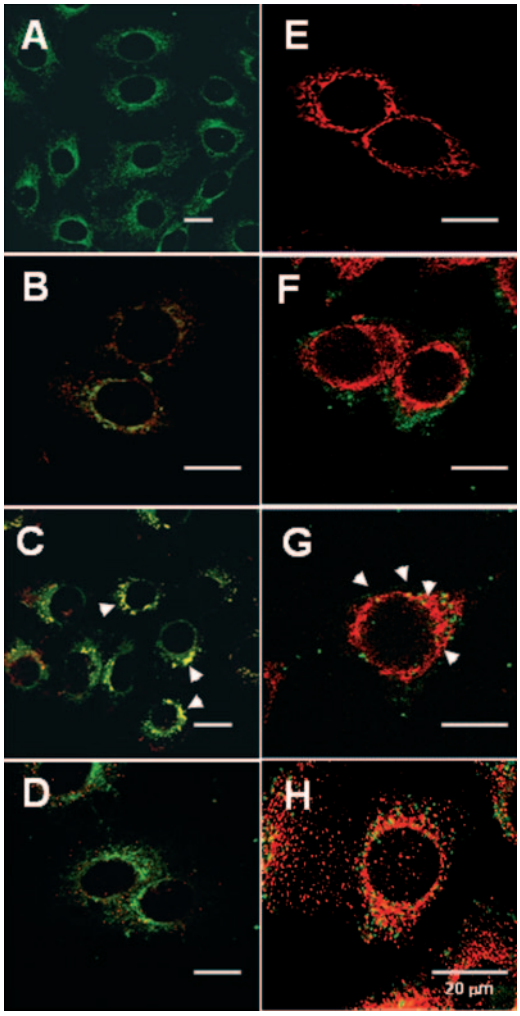

FIG. 4. Pet trafficking to the Golgi apparatus and ER. (A to D) Untreated HEp-2 cells (A) and HEp-2 cells incubated with rhodamine-conjugated Pet (37 μg/ml) (red) for 15 min (B), 30 min (C), or 60 min (D) were fixed, permeabilized, and stained with BODIPY FL C5-ceramide complexed to bovine serum albumin (green). Merged images are shown. The arrowheads indicate the distribution of Golgi apparatus-localized Pet. (E to H) Untreated HEp-2 cells (E) and HEp-2 cells incubated with 37 μg Pet/ml for 30 min (F), 45 min (G), or 60 min (H) were fixed and permeabilized. Pet was visualized with a combination of rabbit anti-Pet antibodies and secondary fluorescein-labeled goat anti-rabbit IgG antibodies (green), while the ER was visualized with a combination of mouse anti-calnexin antibodies and secondary rhodamine-labeled goat anti-mouse IgG antibodies (red). Merged images are shown. The arrowheads indicate the distribution of ER-localized Pet.

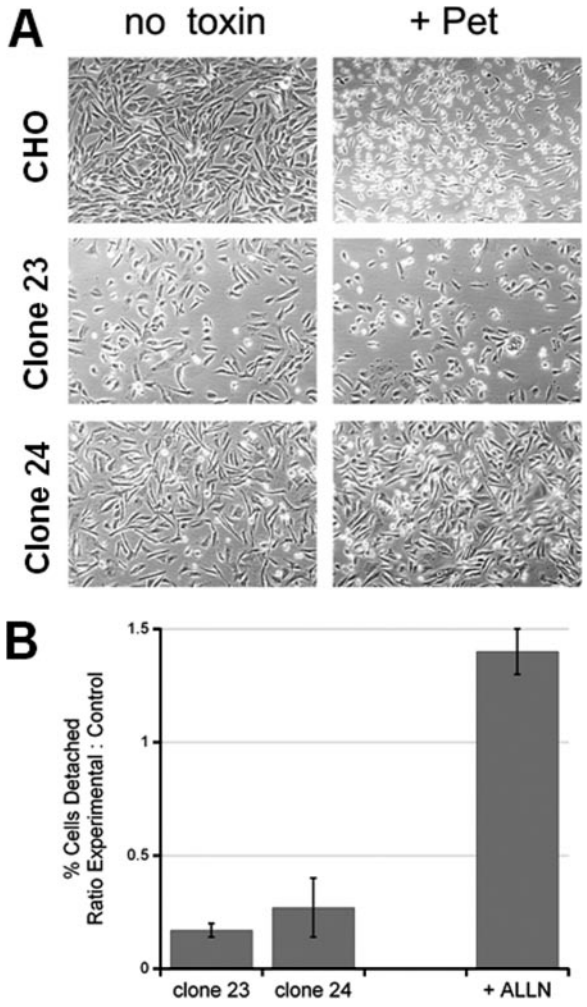

FIG. 5. ERAD dysfunction blocks Pet intoxication. (A) Wild-type CHO cells and two mutant CHO cell lines with ERAD dysfunction (clones 23 and 24) were incubated for 10 h in the absence or presence of 40 μg Pet/ml. Images were taken at a magnification of ×10. (B) Wild-type CHO cells, mutant clone 23, mutant clone 24, and wild-type CHO cells treated with 10 μM of the proteasome inhibitor ALLN were exposed to 40 μg Pet/ml for 20 h. The percentage of detached cells was then determined for each condition. The results are expressed as the ratio of the experimental value to the control value, where the experimental value is the percentage of detached cells from the mutant cell line or ALLN-treated cells and the control value is the percentage of detached cells from the wild-type CHO cells. The averages ± standard deviations of three (mutant cell lines) or five (ALLN treatment) independent experiments are shown.

experiments were performed (Fig. 4). HEp-2 cells exposed to Pet for 30, 45, or 60 min were fixed, permeabilized, and incubated with antibodies against Pet and the resident ER protein calnexin. FITC-labeled secondary antibodies were used to visualize Pet, while TRITC-labeled secondary antibodies were used to visualize calnexin. In control cells that were not exposed to Pet, the ER appeared to be a tubuloreticular halo around the nucleus, as determined by confocal microscopy of sections (Fig. 4E). This staining pattern was not altered by toxin treatment (Fig. 4F to H). After 30 min of intoxication, Pet was found in punctuate structures that did not correspond to the ER (Fig. 4F). However, the toxin did colocalize with calnexin after 45 min of incubation (Fig. 4G). Pet no longer colocalized with calnexin after 60 min of intoxication (Fig. 4H).

The data in Fig. 1 to 4 provide a roadmap for Pet trafficking from the cell surface to early endosomes, from early endosomes to the Golgi apparatus, and from the Golgi apparatus to the ER. After reaching the ER, Pet must be translocated to the cytosol in order to interact with its fodrin target (1).

Translocation of Pet into the cytosol. Many plant and bacterial toxins exploit the ERAD system in order to move from the ER to the cytosol (19, 28). To examine the role of ERAD

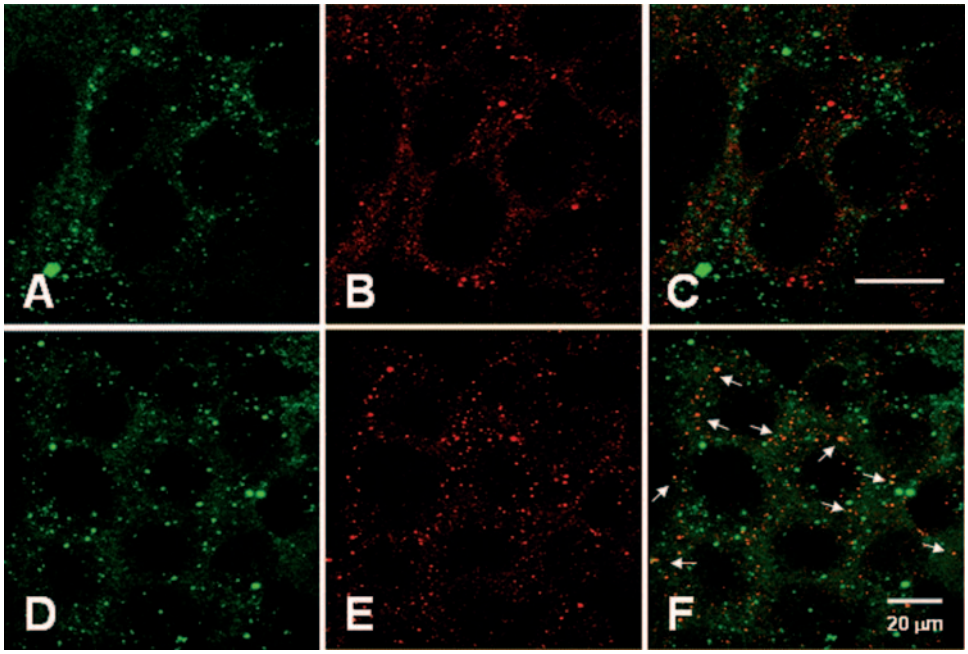

FIG. 6. Colocalization of Pet with the Sec61p translocon. HEp-2 cells incubated with 37 μg Pet/ml for 30 min (A to C) or 55 min (D to F) were fixed and permeabilized. Pet was visualized with a combination of mouse anti-Pet antibodies and secondary fluorescein-labeled goat anti-mouse IgG antibodies (A and D), while Sec61α was visualized with a combination of rabbit anti-Sec61α antibodies and secondary Cy5-labeled goat anti-rabbit IgG antibodies (B and E). Merged images are shown in panels C and F. The arrows indicate sites of protein colocalization.

in Pet intoxication, Pet was added to the extracellular media of wild-type CHO cells and mutant CHO cells with aberrant ERAD activity. Compared to the wild-type parental CHO cells, CHO mutant clones 23 and 24 have elevated levels of ERAD activity that correspond to elevated levels of resistance to three AB-type, ER-translocating toxins: CT, *Pseudomonas aeruginosa* exotoxin A, and ricin (34). The toxin resistance in the mutant cells is due to increased coupling efficiency between translocation and degradation which prevents toxin accumulation in the cytosol. Compared to the wild-type cells, mutant clones 23 and 24 also exhibited substantial resistance to Pet intoxication (Fig. 5). Whereas cell rounding was observed in the wild-type CHO cells after 10 h of incubation with 40 μg Pet/ml, there was only a minimal effect on the morphology of clone 23 or 24 (Fig. 5A). This qualitative observation was supported by the results of quantification of Pet-induced cell detachment after exposure to the toxin for 20 h; many of the wild-type cells but few of the mutant cells had detached from the substratum after 20 h of intoxication (Fig. 5B). However, cell rounding was observed in clones 23 and 24 after 20 h of intoxication (not shown). Thus, ERAD dysfunction in clones 23 and 24 appeared to effectively delay the onset of Pet intoxication.

ER-translocating toxins evade the ubiquitin-proteasome system, although proteasomal inhibition can result in mild sensitization to some ER-translocating toxins, such as ricin (37). To determine whether proteasomal inhibition could affect Pet intoxication, CHO cells were incubated with 40 μg Pet/ml for 20 h in the absence or presence of the proteasome inhibitor ALLN. Cells exposed to 10 μM ALLN were more susceptible to Pet intoxication than cells incubated in the absence of ALLN were (Fig. 5B). This indicated that at least a percentage of translocated Pet is susceptible to proteasome-mediated degradation in the cytosol. Cells exposed to 10 μM ALLN alone did not exhibit substantial cell detachment (not shown) and were used to normalize the detachment results obtained with CHO cells incubated with both Pet and ALLN.

AB toxins and other ERAD substrates can be exported to the cytosol through the Sec61p translocon (17, 27, 28). To investigate the role of Sec61p in Pet translocation, we performed colocalization experiments with Pet and the largest subunit of the heterotrimeric Sec61 complex, Sec61α (Fig. 6). After 30 or 55 min of incubation with Pet, HEp-2 cells were fixed, permeabilized, and incubated with antibodies against Pet and Sec61α. FITC-labeled secondary antibodies were used to visualize Pet, while TRITC-labeled secondary antibodies were used to visualize Sec61α. Confocal microscopy showed that Pet did not colocalize with Sec61α after 30 min of intoxication (Fig. 6A to C). However, Pet colocalization with Sec61α was readily apparent after 55 min of incubation (Fig. 6D to F). These data indicated that Pet associates with the Sec61p translocon before passage into the cytosol.

To confirm the interaction between Pet and Sec61α, coimmunoprecipitation experiments were performed with Pet-treated and untreated cells. Antibodies against Sec61α were able to precipitate Pet in Pet-treated cells but not in untreated cells (Fig. 7A). Similarly, as expected, antibodies against Pet were able to precipitate Pet in Pet-treated cells but not in untreated cells; a positive control showed that the purified Pet protein was immunoprecipitated with the anti-Pet antibodies (Fig. 7A). To determine at what time the two proteins interact with each other, coimmunoprecipitation experiments were performed after 30, 60, and 75 min of Pet intoxication (Fig. 7B), which were times used in the previous immunocytochem-

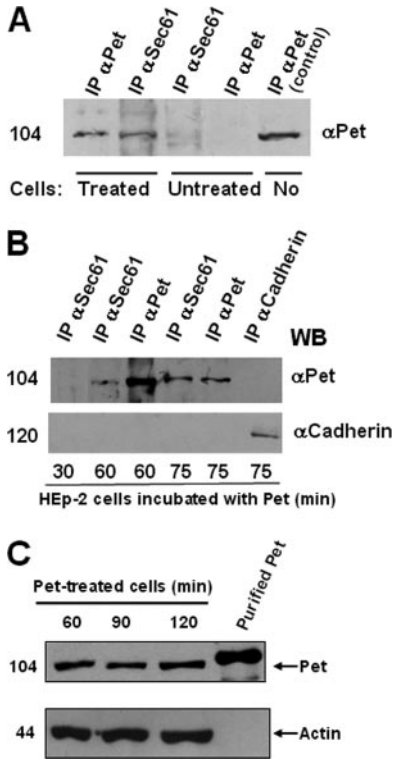

FIG. 7. Pet and Sec61p interaction and full-length Pet translocation. (A and B) Coimmunoprecipitation of Pet and the Sec61p translocon. (A) Coimmunoprecipitation of Pet by using antibodies against Sec61α or Pet in cells treated with Pet for 1 h or in untreated cells. IP, immunoprecipitation. (B) Coimmunoprecipitation at various times. HEp-2 cells incubated with 37 μg Pet/ml for 30, 60, or 75 min were lysed, and the resulting supernatants were immunoprecipitated with either anti-Sec61α, anti-Pet, or anti-cadherin antibodies. A Western blot analysis of the immunoprecipitated proteins was conducted with anti-Pet antibodies, followed by a secondary peroxidase-labeled antibody. The position of a molecular weight marker is indicated on the left. (C) Pet detection in cytoplasmic fractions from Pet-treated cells. HEp-2 cells incubated with 37 μg Pet/ml for 60, 90, or 120 min were lysed and ultracentrifuged, and soluble cytoplasmic fractions were obtained. Equivalent volumes of the samples were subjected to SDS-PAGE, transferred to nitrocellulose membranes, and probed with a rabbit anti-Pet polyclonal antibody (top). Protein loading was monitored by stripping and reprobing with a mouse monoclonal anti-actin antibody (bottom).

ical experiments (Fig. 6). Antibodies against Sec61α were used to precipitate the Pet-Sec61 complex. After 30 min of intoxication, Pet was not detected in the Sec61α immunoprecipitate. This negative result demonstrated the specificity of the Pet-Sec61α interaction that was detected by Sec61α immunoprecipitation after 60 and 75 min of intoxication. Pet was not detected by immunoprecipitation with an irrelevant antibody against the cell adhesion molecule cadherin (Fig. 7B). These data confirmed the results of the colocalization studies shown in Fig. 6 and demonstrated that after 1 h of trafficking from the cell surface to the ER, full-length Pet was able to associate with the Sec61p translocon. The interaction of full-length Pet with Sec61α also suggested that the entire toxin could be translocated into the cytosol.

All the established ER-translocating toxins undergo AB subunit dissociation before A-chain passage into the cytosol. Since Pet is not an AB toxin, the possible processing after translocation was verified by detecting the molecular mass of the Pet protein. HEp-2 cells were treated with Pet for 60, 90, and 120 min, and cellular fractions were obtained from these cells. Anti-Pet antibodies showed that the cytoplasmic fractions from Pet-treated cells contained Pet protein as a 104-kDa protein from 60 min of incubation, and it remained present during the long times tested (90 and 120 min) (Fig. 7C). Differences in migration and protein loading were controlled by detecting actin in the same nitrocellulose membrane obtained from the 8% SDS–PAGE gel probed with anti-actin antibodies (Fig. 7C).

Thus, these results and the results obtained by coimmunoprecipitating Pet and Sec61 suggest that Pet is the largest bacterial toxin reported to date that translocates from the ER by a retrograde pathway and that even if there is some processing, there is not a great deal of processing.

DISCUSSION

Many AB toxins move from the cell surface to the ER before accessing the host cell cytosol (19, 28). There are a variety of retrograde trafficking pathways to the ER, and the route(s) followed by a particular toxin appears to be dictated by the association of the toxin B subunit with its specific host receptor(s). However, all these ER-translocating toxins undergo AB subunit dissociation before A-chain passage into the cytosol. Most, if not all, of the ER-translocating toxins also utilize ERAD and the Sec61p translocon to move from the lumen of the endomembrane system to the cytosol (27). By following the intracellular trafficking and translocation of Pet, a non-AB toxin, we have shown that an AB structural organization is not required for toxin trafficking to the ER and toxin translocation to the cytosol.

The aim of this work was to identify the mechanism of Pet trafficking in intoxicated cells. We have recently documented Pet binding to the epithelial cell surface, clathrin-dependent Pet endocytosis, and productive Pet intoxication in the absence of functional lipid rafts (Navarro-Garcia et al. submitted). Lipid rafts are involved in the intracellular trafficking of many ER-translocating toxins, but this association varies from toxin to toxin and does not appear to be essential for Pet activity against epithelial cells. Pet intoxication was also not affected by treatment with NH_4Cl. This indicated that Pet does not use the acidified endosomes as a translocation site for entry into the cytosol. However, wortmannin-treated cells were very resistant to Pet. The disruption of PI 3-kinase activity by wortmannin has a number of negative effects on vesicle transport, including alterations in (i) passage of the transferrin receptor through the endocytic pathway (33), (ii) incorporation of the calcium-independent mannose-6-phosphate receptor into trans-Golgi network-derived clathrin-coated vesicles (6), (iii) trafficking of the bradykinin B2 receptor (12), and (iv) movement of ricin from the early endosomes to the Golgi apparatus (16, 20). Thus, the inhibitory effect of wortmannin on Pet intoxication suggests that PI 3-kinase has a functional role in the endocytic vesicular transport of Pet.

Pet endocytosis was rapid in HEp-2 cells, and Pet was found in the early endosomes after 8 min of exposure to the toxin; this colocalization was inhibited at 4°C (data not shown). Ef-

ficient endocytosis and rapid toxin delivery to the early endosomes by either clathrin-dependent or clathrin-independent mechanisms have been documented for numerous AB-type toxins as well (31). A fraction of internalized Pet was delivered to the lysosomes, which has also been observed for AB-type toxins (29). However, the functional pool of Pet was directed to other organelles.

Our studies indicate that Pet has the same general trafficking itinerary that many established AB-type, ER-translocating toxins have. In previous work, we found that BfA inhibited Pet-induced disruption of the actin cytoskeleton (22). Inhibition of cell intoxication by BfA has been observed for ER-translocating toxins such as CT, Shiga toxin, and ricin (3, 25, 40). This suggested that Pet is also an ER-translocating toxin, but the additional effects of BfA on endocytic traffic prevented a definitive conclusion to be made concerning the intracellular trafficking route of Pet. In this work, we verified Pet trafficking to the Golgi apparatus and ER. Confocal microscopy documented the sequential movement of Pet to the Golgi apparatus after 30 min of toxin exposure and to the ER after 45 min of toxin exposure. This rate of transport is similar to the rates that have been observed for the Golgi apparatus/ER trafficking of other ER-translocating toxins (25, 36). Pet lacks a C-terminal KDEL or RDEL ER retrieval motif, so its retrograde transport to the ER may occur by a COP-1-independent mechanism like that observed for Shiga toxin and ricin (2, 7). The orderly movement of Pet from the endosomes to the Golgi apparatus and from the Golgi apparatus to the ER strongly suggested that the ER is the translocation site for Pet.

The ER is an attractive compartment for toxin translocation, as it contains numerous factors that can facilitate protein passage into the cytosol. One of these factors is the Sec61p translocon, a gated pore in the ER membrane that is involved in the ERAD-mediated export of misfolded proteins from the ER lumen to the cytosol (38). Here we documented that there is a physical association between full-length Pet and Sec61α, a major component of the Sec61p translocon complex. Likewise, the A chains of CT (30), ETA (15), and ricin (37) have been shown to interact physically or functionally with the translocon. Colocalization of Pet and Sec61α in discrete regions of the ER was further demonstrated by confocal microscopy. These discrete regions may represent the putative ER exit sites described for Shiga-like toxin 1 (32) and two other ERAD substrates, the precursor of human asialoglycoprotein receptor H2a and the free heavy chain of the class I major histocompatibility complex (14). Interestingly, the ER distribution of H2a did not completely coincide with the distribution of the ER resident protein BiP (14). Segregation of ERAD substrates into ER subdomain exit sites may explain the different distributions of Pet and calnexin after 60 min of intoxication, a time at which Pet was still associated with the ER and the Sec61p translocon. Finally, a functional role for the ERAD system in Pet intoxication was established by using two mutant CHO cell lines that exhibit elevated levels of ERAD activity and elevated levels of resistance to CT, ETA, and ricin (34). Pet and the ER-translocating AB toxins thus appear to have similar ER-to-cytosol export mechanisms that involve both ERAD and the Sec61p translocon.

Although Pet and the ER-translocating AB toxins follow similar intracellular trafficking and translocation pathways, our work revealed a unique aspect of Pet intoxication: the entire 104-kDa Pet protein was translocated into the cytosol. Full-length Pet was detected in the cytoplasmic fraction of Pet-treated cells, which was separated by 8% SDS–PAGE. This is in marked contrast to AB toxin translocation, as AB subunit dissociation precedes or occurs concurrent with A chain passage into the cytosol. AB toxin processing in the pathogen or target cell generates a structural state which facilitates holotoxin disassembly in the environmental conditions of the ER lumen. The dissociated A chain then masquerades as a misfolded protein in order to promote its ERAD-mediated translocation into the cytosol. The fate of the ER-localized B subunit remains unknown, but it is thought that a main function of the cell-binding B subunit is simply to deliver the A subunit to its translocation site (17). Pet does not fit into this standard model of AB toxin trafficking since it does not dissociate into component parts in the ER and instead can be found in the cytosol as an intact, 104-kDa protein. The presence of full-length Pet in the cytosol suggests that multiple domains of the toxin are required for its cytopathic activity. The large size of translocated Pet (in contrast to the ~20- to 40-kDa translocated toxin A chains) and its export as an intact toxin also suggest that the ERAD-mediated translocation of Pet may be mechanistically distinct from the ERAD-mediated translocation of toxin A chains.

Another difference between Pet and the ER-translocating AB toxins is the abundance of lysine residues in Pet (4). The A chains of ER-translocating toxins exhibit a strong codon bias for arginine over lysine. This is thought to protect the translocated A chain from ubiquitin-dependent proteasomal degradation, as ubiquitin is appended to lysine residues but not to arginine residues (8). The arginine-over-lysine codon bias is not found in the toxin B subunits and is not found in Pet. This suggests that translocated Pet could be readily degraded by the ubiquitin-proteasome system. This possibility is supported by the Pet-resistant phenotype of the mutant cell lines with elevated levels of ERAD activity. The observed sensitization to Pet upon proteasomal inhibition is also consistent with the hypothesis that the proteasome has a functional role in Pet degradation. Sensitization was achieved with a suboptimal concentration of ALLN (higher inhibitor concentrations were toxic during prolonged incubations), and the level of sensitization was similar to the ~3-fold level of ricin sensitization observed in cells treated with a proteasome inhibitor (37). Efficient toxin degradation in the cytosol could explain, in part, why such high concentrations of Pet are required to elicit toxic effects.

Pet is the first SPATE and the first non-AB bacterial toxin with demonstrated trafficking to the ER and demonstrated translocation from the ER to the cytosol. Collectively, our work has shown that the interaction of Pet with the target cell involves a discrete series of events, including (i) binding to the cell surface; (ii) uptake into the cell by a clathrin-dependent endocytic mechanism that does not require lipid rafts; (iii) entry into early endosomes; (iv) transfer from endosomes to the Golgi apparatus; (v) retrograde vesicular transport from the Golgi complex to the ER; (vi) translocation of the entire toxin to the cytosol, possibly by the ER-associated degradation pathway; and (vii) cleavage of fodrin to induce cytoskeletal damage (1, 24). The *pet* gene thus contains all the necessary

information to mediate toxin autosecretion from *E. coli*, toxin internalization and trafficking in the host cell, toxin translocation into the host cell cytosol, and toxin damage to the host cell cytoskeleton via fodrin cleavage.

ACKNOWLEDGMENTS

This work was supported by grants from Consejo Nacional de Ciencia y Tecnología de México (CONACYT grants 30004 M and C02-44660) to F.N.-G. and by NIH grant K22 AI054568 to K.T.

We also thank Rocio Huerta and Sandra Geden for technical help.

REFERENCES

1. **Canizalez-Roman, A., and F. Navarro-Garcia.** 2003. Fodrin CaM-binding domain cleavage by Pet from enteroaggregative *Escherichia coli* leads to actin cytoskeletal disruption. Mol. Microbiol. **48:**947–958.
2. **Chen, A., R. J. AbuJarour, and R. K. Draper.** 2003. Evidence that the transport of ricin to the cytoplasm is independent of both Rab6A and COPI. J. Cell Sci. **116:**3503–3510.
3. **Donta, S. T., T. K. Tomicic, and A. Donohue-Rolfe.** 1995. Inhibition of Shiga-like toxins by brefeldin A. J. Infect. Dis. **171:**721–724.
4. **Eslava, C., F. Navarro-Garcia, J. R. Czeczulin, I. R. Henderson, A. Cravioto, and J. P. Nataro.** 1998. Pet, an autotransporter enterotoxin from enteroaggregative *Escherichia coli*. Infect. Immun. **66:**3155–3163.
5. **Fernandez-Borja, M., R. Wubbolts, J. Calafat, H. Janssen, N. Divecha, S. Dusseljee, and J. Neefjes.** 1999. Multivesicular body morphogenesis requires phosphatidyl-inositol 3-kinase activity. Curr. Biol. **9:**55–58.
6. **Gaffet, P., A. T. Jones, and M. J. Clague.** 1997. Inhibition of calcium-independent mannose 6-phosphate receptor incorporation into trans-Golgi network-derived clathrin-coated vesicles by wortmannin. J. Biol. Chem. **272:** 24170–24175.
7. **Girod, A., B. Storrie, J. C. Simpson, L. Johannes, B. Goud, L. M. Roberts, J. M. Lord, T. Nilsson, and R. Pepperkok.** 1999. Evidence for a COP-I-independent transport route from the Golgi complex to the endoplasmic reticulum. Nat. Cell Biol. **1:**423–430.
8. **Hazes, B., and R. J. Read.** 1997. Accumulating evidence suggests that several AB-toxins subvert the endoplasmic reticulum-associated protein degradation pathway to enter target cells. Biochemistry **36:**11051–11054.
9. **Henderson, I. R., and J. P. Nataro.** 2001. Virulence functions of autotransporter proteins. Infect. Immun. **69:**1231–1243.
10. **Henderson, I. R., F. Navarro-Garcia, M. Desvaux, R. C. Fernandez, and D. Ala'Aldeen.** 2004. Type V protein secretion pathway: the autotransporter story. Microbiol. Mol. Biol. Rev. **68:**692–744.
11. **Henderson, I. R., F. Navarro-Garcia, and J. P. Nataro.** 1998. The great escape: structure and function of the autotransporter proteins. Trends Microbiol. **6:**370–378.
12. **Houle, S., and F. Marceau.** 2003. Wortmannin alters the intracellular trafficking of the bradykinin B2 receptor: role of phosphoinositide 3-kinase and Rab5. Biochem. J. **375:**151–158.
13. **Jones, A. T., and M. J. Clague.** 1995. Phosphatidylinositol 3-kinase activity is required for early endosome fusion. Biochem. J. **311:**31–34.
14. **Kamhi-Nesher, S., M. Shenkman, S. Tolchinsky, S. V. Fromm, R. Ehrlich, and G. Z. Lederkremer.** 2001. A novel quality control compartment derived from the endoplasmic reticulum. Mol. Biol. Cell **12:**1711–1723.
15. **Koopmann, J. O., J. Albring, E. Huter, N. Bulbuc, P. Spee, J. Neefjes, G. J. Hammerling, and F. Momburg.** 2000. Export of antigenic peptides from the endoplasmic reticulum intersects with retrograde protein translocation through the Sec61p channel. Immunity **13:**117–127.
16. **Lauvrak, S. U., A. Llorente, T. G. Iversen, and K. Sandvig.** 2002. Selective regulation of the Rab9-independent transport of ricin to the Golgi apparatus by calcium. J. Cell Sci. **115:**3449–3456.
17. **Lencer, W. I., and B. Tsai.** 2003. The intracellular voyage of cholera toxin: going retro. Trends Biochem. Sci. **28:**639–645.
18. **Li, G., C. D'Souza-Schorey, M. A. Barbieri, R. L. Roberts, A. Klippel, L. T. Williams, and P. D. Stahl.** 1995. Evidence for phosphatidylinositol 3-kinase as a regulator of endocytosis via activation of Rab5. Proc. Natl. Acad. Sci. USA **92:**10207–10211.
19. **Lord, J. M., and L. M. Roberts.** 1998. Toxin entry: retrograde transport through the secretory pathway. J. Cell Biol. **140:**733–736.
20. **Mallet, W. G., and F. R. Maxfield.** 1999. Chimeric forms of furin and TGN38 are transported with the plasma membrane in the trans-Golgi network via distinct endosomal pathways. J. Cell Biol. **146:**345–359.
21. **Moskaug, J. O., K. Sandvig, and S. Olsnes.** 1988. Low pH-induced release of diphtheria toxin A-fragment in Vero cells. Biochemical evidence for transfer to the cytosol. J. Biol. Chem. **263:**2518–2525.
22. **Navarro-Garcia, F., A. Canizalez-Roman, J. Luna, C. Sears, and J. P. Nataro.** 2001. Plasmid-encoded toxin of enteroaggregative *Escherichia coli* is internalized by epithelial cells. Infect. Immun. **69:**1053–1060.
23. **Navarro-Garcia, F., C. Eslava, J. M. Villaseca, R. Lopez-Revilla, J. R. Czeczulin, S. Srinivas, J. P. Nataro, and A. Cravioto.** 1998. In vitro effects of a high-molecular-weight heat-labile enterotoxin from enteroaggregative *Escherichia coli*. Infect. Immun. **66:**3149–3154.
24. **Navarro-Garcia, F., C. Sears, C. Eslava, A. Cravioto, and J. P. Nataro.** 1999. Cytoskeletal effects induced by Pet, the serine protease enterotoxin of enteroaggregative *Escherichia coli*. Infect. Immun. **67:**2184–2192.
25. **Orlandi, P. A., P. K. Curran, and P. H. Fishman.** 1993. Brefeldin A blocks the response of cultured cells to cholera toxin. Implications for intracellular trafficking in toxin action. J. Biol. Chem. **268:**12010–12016.
26. **Ratts, R., C. Trujillo, A. Bharti, J. vander Spek, R. Harrison, and J. R. Murphy.** 2005. A conserved motif in transmembrane helix 1 of diphtheria toxin mediates catalytic domain delivery to the cytosol. Proc. Natl. Acad. Sci. USA **102:**15635–15640.
27. **Romisch, K.** 1999. Surfing the Sec61 channel: bidirectional protein translocation across the ER membrane. J. Cell Sci. **112:**4185–4191.
28. **Sandvig, K., and B. van Deurs.** 2005. Delivery into cells: lessons learned from plant and bacterial toxins. Gene Ther. **12:**865–872.
29. **Sandvig, K., and B. van Deurs.** 1996. Endocytosis, intracellular transport, and cytotoxic action of Shiga toxin and ricin. Physiol. Rev. **76:**949–966.
30. **Schmitz, A., H. Herrgen, A. Winkeler, and V. Herzog.** 2000. Cholera toxin is exported from microsomes by the Sec61p complex. J. Cell Biol. **148:**1203–1212.
31. **Simpson, J. C., D. C. Smith, L. M. Roberts, and J. M. Lord.** 1998. Expression of mutant dynamin protects cells against diphtheria toxin but not against ricin. Exp. Cell Res. **239:**293–300.
32. **Smith, D. C., D. J. Sillence, T. Falguieres, R. M. Jarvis, L. Johannes, J. M. Lord, F. M. Platt, and L. M. Roberts.** 2006. The association of Shiga-like toxin with detergent-resistant membranes is modulated by glucosylceramide and is an essential requirement in the endoplasmic reticulum for a cytotoxic effect. Mol. Biol. Cell **17:**1375–1387.
33. **Spiro, D. J., W. Boll, T. Kirchhausen, and M. Wessling-Resnick.** 1996. Wortmannin alters the transferrin receptor endocytic pathway in vivo and in vitro. Mol. Biol. Cell **7:**355–367.
34. **Teter, K., M. G. Jobling, and R. K. Holmes.** 2003. A class of mutant CHO cells resistant to cholera toxin rapidly degrades the catalytic polypeptide of cholera toxin and exhibits increased endoplasmic reticulum-associated degradation. Traffic **4:**232–242.
35. **Towbin, H., T. Staehelin, and J. Gordon.** 1979. Electrophoretic transfer of proteins from polyacrylamide gels to nitrocellulose sheets: procedure and some applications. Proc. Natl. Acad. Sci. USA **76:**4350–4354.
36. **van Deurs, B., K. Sandvig, O. W. Petersen, S. Olsnes, K. Simons, and G. Griffiths.** 1988. Estimation of the amount of internalized ricin that reaches the trans-Golgi network. J. Cell Biol. **106:**253–267.
37. **Wesche, J., A. Rapak, and S. Olsnes.** 1999. Dependence of ricin toxicity on translocation of the toxin A-chain from the endoplasmic reticulum to the cytosol. J. Biol. Chem. **274:**34443–34449.
38. **Wiertz, E. J., D. Tortorella, M. Bogyo, J. Yu, W. Mothes, T. R. Jones, T. A. Rapoport, and H. L. Ploegh.** 1996. Sec61-mediated transfer of a membrane protein from the endoplasmic reticulum to the proteasome for destruction. Nature **384:**432–438.
39. **Wurmser, A. E., J. D. Gary, and S. D. Emr.** 1999. Phosphoinositide 3-kinases and their FYVE domain-containing effectors as regulators of vacuolar/lysosomal membrane trafficking pathways. J. Biol. Chem. **274:**9129–9132.
40. **Yoshida, T., C. C. Chen, M. S. Zhang, and H. C. Wu.** 1991. Disruption of the Golgi apparatus by brefeldin A inhibits the cytotoxicity of ricin, modeccin, and *Pseudomonas* toxin. Exp. Cell Res. **192:**389–395.

Editor: A. D. O'Brien